

# Molecular assemblies of novel amphiphilic phthalocyanines: an investigation into the self-ordering properties of complex functional materials

Ziad Ali-Adib,<sup>a</sup> Guy J. Clarkson,<sup>a</sup> Neil B. McKeown,<sup>\*a,†</sup> Kevin E. Treacher,<sup>a</sup> Helen F. Gleeson<sup>b</sup> and Alexander S. Stennett<sup>b</sup>

<sup>a</sup>Department of Chemistry, University of Manchester, UK M13 9PL

<sup>b</sup>Department of Physics and Astronomy, University of Manchester, UK M13 9PL

Received 17th July 1998, Accepted 18th August 1998

The synthesis and liquid crystalline properties of unsymmetrically substituted Pcs which contain both alkyl and hydroxy terminated tetra(ethyleneoxy) side-chains are described. Despite poor Langmuir–Blodgett film forming properties, the amphiphilic Pcs are of interest as they display a variety of columnar mesophases and the ability to form self-ordered lamellar films by simple solvent casting. Lamellar order can be obtained in spin-coated films of these derivatives by annealing at a temperature at which the Pc is liquid crystalline. These self-ordering spin-coated films are an alternative to the laborious Langmuir–Blodgett technique for the fabrication of highly ordered and uniform films of functional molecular materials.

In order to exploit the electronic or optical properties of functional compounds it is necessary to understand, predict and control the structure of their condensed states. Since their discovery seventy years ago, phthalocyanines (Pcs) have become one of the most studied of all organic functional materials. In addition to their use as blue and green colorants, Pcs are of increasing interest for applications in non-linear optics, xerography, molecular electronics, photodynamic cancer therapy, solar energy conversion, catalysis and as the active component of gas sensors.<sup>1</sup> Much is now known about the structures of the various crystalline polymorphs of Pc and its metal ion containing derivatives.<sup>1a</sup> However, in order to optimise their potential utility in electronic and optoelectronic devices, it is necessary to fabricate Pcs as thin films in which the nano-scale architecture and ordering can be reproducibly controlled. Vacuum sublimation<sup>1a,2</sup> or the spin-coating of Pc particles dispersed in a soluble polymer matrix<sup>1a,3</sup> remain the most important techniques for the fabrication of films derived from these insoluble compounds. However, research into the synthesis of substituted Pcs has provided materials which are soluble and therefore suitable for film fabrication by the Langmuir–Blodgett (LB) technique<sup>1a,4</sup> or by the spin-coating of pure material.<sup>1a,5</sup> In addition, suitable substitution of the Pc macrocycle by flexible side-chains, either alkyl or oligo(ethyleneoxy), gives materials which self-order to form columnar mesophases.<sup>1,6</sup> The external control over molecular orientation afforded by liquid crystallinity may enable the fabrication of monodomain, ordered solid films.

This paper describes the synthesis and self-ordering properties of unsymmetrically substituted Pcs which contain both alkyl (hexadecyl) and hydroxy terminated tetra(ethyleneoxy) side-chains. These Pcs were originally designed as amphiphilic materials for deposition as LB multilayer films, and their monolayer forming properties and failed attempts to prepare LB films are described. Interestingly, it was discovered that they display a variety of thermotropic columnar mesophases and the ability to form self-ordered multilayer (lamellar) films by simple solvent casting.<sup>7</sup> Therefore, it was of interest to determine whether highly-ordered spin-coated films, of uniform thickness, could be obtained from these materials and to re-examine in more detail the relationship

between their liquid crystalline behaviour and the formation of ordered films. The liquid crystalline properties of the trityl-protected precursors are also described.

## Experimental

### Liquid crystal characterisation

Differential scanning calorimetry measurements were made on a Seiko DSC 220C machine and calibrated using an indium standard. Optical microscopy observations were made on a Nikon Optiphot-2 microscope with a Mettler FP80 HT Hot Stage. Photographs of the optical textures [Fig. 1(a)–(e)] were taken using the same arrangement equipped with a Nikon FX-35 W camera. Low resolution X-ray diffraction (XRD) from powder samples was recorded using Cu-K $\alpha$  radiation ( $\lambda = 1.54 \text{ \AA}$ ) from a Philips PW1130/00 generator with a nickel filter. The samples were contained in glass capillaries (Hilgenberg 0.01 mm thick glass, 1.0 mm outside diameter X-ray capillaries) and placed in the beam in an aluminium heating block. The temperature was regulated by a Control Techniques Process Instruments 453 Plus Thermal Controller. The diffracted X-rays were detected with a flat-plate photographic camera using Agfa-Gevaert Osray M3 X-ray film. The system was calibrated using sodium chloride. High resolution XRD analysis was carried out using the synchrotron radiation source (SRS) at Daresbury (Station 8.2,  $\lambda = 1.54 \text{ \AA}$ ) using previously described methods for data collection and manipulation.<sup>8</sup> The X-ray camera at the SRS was calibrated with collagen and both small and wide angle scattering data were collected. The high X-ray flux available at the SRS allowed XRD patterns to be obtained rapidly, typically in just a few minutes, enabling data to be collected at different temperatures without any danger of sample degradation.

### Langmuir film characterisation

Isotherm behaviour was measured for monolayers, spread from chloroform (Aldrich, HPLC grade) solution, on pure water at pH 5.5 with no added ions using the apparatus and procedures described previously.<sup>9</sup> Multilayer film formation was attempted on clean glass slides appropriately treated to provide either hydrophilic or hydrophobic surfaces.

†E-mail: neil.mckeown@man.ac.uk

## Film fabrication and characterisation

Solvent cast films and spin-coated films were prepared from the same chloroform solutions ( $\sim 0.02 \text{ g ml}^{-1}$ ). The substrates were clean silicon or glass microscope slides pre-treated with hexamethyldisilazane vapour. Spin-coating was achieved, at 5000 rpm, using a Headway Research Inc. PM80 wafer spin cleaner. Glancing angle X-ray diffraction from the films was recorded using Cu-K $\alpha$  radiation in a Philips PW1050 X-ray Diffractometer using a rotating intensity detector.

## Pc synthesis and structural characterisation

Routine  $^1\text{H}$  NMR spectra were measured at 300 MHz using an Inova 300 spectrometer. High resolution (500 MHz)  $^1\text{H}$  NMR spectra were recorded using a Varian Unity 500 spectrometer. UV-Visible spectra were recorded on a Shimadzu UV-260 spectrophotometer using cells of pathlength 10 mm. IR spectra were recorded on an ATI Mattson Genesis Series FTIR (KBr/Germanium beam splitter). Elemental analyses were obtained using a Carlo Erba Instruments CHNS-O EA 108 Elemental Analyser. Routine low resolution chemical ionisation (CI) and electron ionisation (EI) were obtained using a Fisons Instruments Trio 2000. Fast atom bombardment (FAB) spectra were recorded on a Kratos Concept spectrometer. All solvents were dried and purified as described in Perrin and Armarego.<sup>10</sup> Silica gel (60 Merck 9385) was used in the separation and purification of compounds by column chromatography. All Pcs were heated at 120–150 °C under vacuum for 18 h as the final step of purification.

### 4-(14,14,14-Triphenyl-1,4,7,10,13-pentaoxatetradecyl)phthalonitrile 1

To a solution of 4-nitrophthalonitrile (1.4 g, 8.0 mmol, Aldrich) and tetraethylene glycol monotrityl ether<sup>11</sup> (3.4 g, 8.0 mmol) in anhydrous DMF (30 ml) was added anhydrous potassium carbonate (2 g, 14.5 mmol) and the mixture stirred under nitrogen for 6 days at 50 °C. Water was added (100 ml) and the mixture extracted with Et<sub>2</sub>O (3  $\times$  60 ml), washed with water (2  $\times$  50 ml) and dried over anhydrous magnesium sulfate. The solvent was removed and the product recrystallised from hexane-toluene (2:1) to give **1** as colourless plates (2.1 g, 47%), mp 92–94 °C;  $\nu$  (KBr)/cm<sup>-1</sup> 2230 (C $\equiv$ N) (Found C, 74.55; H, 6.41; N, 5.02%. C<sub>35</sub>H<sub>34</sub>N<sub>2</sub>O<sub>5</sub> requires C, 74.71; H, 6.09; N, 4.98%);  $\delta_{\text{H}}$  (200 MHz, CDCl<sub>3</sub>) 3.21 (t, 2H), 3.64–3.70 (m, 10H), 3.84 (t, 2H), 4.04 (t, 2H), 7.05 (dd, 1H), 7.10 (d, 1H), 7.19 (t, 3H), 7.26 (t, 6H), 7.45 (d, 6H), 7.57 (d, 1H);  $m/z$  (CI) 580 (M<sup>+</sup> + NH<sub>4</sub><sup>+</sup>).

### Phthalocyanines 2–7

To a rapidly stirred mixture of compound **1** (2.0 g, 3.55 mmol) and 4,5-bis(hexadecyl)phthalonitrile<sup>6c</sup> (1.9 g, 3.39 mmol) in refluxing pentanol (10 ml), under a nitrogen atmosphere, was added excess lithium metal (0.2 g). Heating and stirring were continued for 6 h. On cooling, water (30 ml) was added and the reaction mixture heated to ensure complete removal of lithium ions from the central cavity of the Pcs. Evaporation of the water, under reduced pressure, left a green product mixture. The resultant solid was dissolved in toluene and passed through a silica column, at 50 °C, using an eluent composed of an increasing amount of THF relative to toluene.

The first fraction (85 mg, 2%) ( $R_f=0.9$ , 50 °C, toluene) proved to be identical to a previously prepared sample of 2,3,9,10,16,17,23,24-octakis(hexadecyl)phthalocyanine **2**.<sup>1g</sup>

The second fraction was collected and applied to a fresh silica column (eluent: toluene-heptane, 1:1, 50 °C,  $R_f=0.5$ ) and recrystallised from heptane to afford 2,3,9,10,16,17-hexakis(hexadecyl)-23-(14,14,14-triphenyl-1,4,7,10,13-pentaoxatetradecyl)phthalocyanine **3** as a blue solid (316 mg, 8%). (Found C, 81.30; H, 10.70; N, 4.89%. C<sub>155</sub>H<sub>240</sub>N<sub>8</sub>O<sub>5</sub> requires C, 81.10;

H; 10.54; N, 4.88%);  $\lambda_{\text{max}}$  (toluene)/nm 706, 670, 644, 606, 350;  $\delta_{\text{H}}$  (500 MHz, C<sub>6</sub>D<sub>6</sub>, 60 °C) -0.6 (br s, 2H), 1.01 (t, 18H), 1.22–1.7 (m, 144H), 1.78 (m, 12H), 2.14 (m, 12H), 3.33 (m, 12H), 3.42 (t, 2H), 3.68 (t, 2H), 3.72 (m, 2H), 3.76 (m, 2H), 3.81–3.86 (m, 4H), 3.97 (br t, 2H), 4.35 (br t, 2H), 7.19 (tt, 3H), 7.70 (dd, 6H), 7.79 (d, 1H), 9.15 (br s, 1H), 9.45–9.77 (br m, 7H);  $m/z$  (FAB) 2298, <sup>13</sup>C<sub>2</sub>C<sub>153</sub>H<sub>240</sub>N<sub>8</sub>O<sub>5</sub> (M<sup>+</sup> + H<sup>+</sup>) requires 2298.

The third fraction was collected and applied to a fresh silica column (eluent: toluene, 20 °C,  $R_f=0.30$ ) and recrystallised from heptane to afford 2,3,16,17-tetrakis(hexadecyl)-16,23(24)-bis(14,14,14-triphenyl-1,4,7,10,13-pentaoxatetradecyl)phthalocyanine **4** as a mixture of two isomers (108 mg, 3%) (Found C, 79.15; H, 9.37; N, 4.86%. C<sub>150</sub>H<sub>206</sub>N<sub>8</sub>O<sub>10</sub> requires C, 78.97; H, 9.10; N, 4.91%);  $\lambda_{\text{max}}$  (toluene)/nm 706, 670, 638, 608, 380, 292;  $\delta_{\text{H}}$  (500 MHz, C<sub>6</sub>D<sub>6</sub>, 60 °C) -1.10 (br s, 2H), 1.00 (br t, 12H), 1.3–1.89 (br m, 104H), 2.10–2.25 (br m, 8H), 3.20–3.43 (br m, 8H), 3.44 (m, 4H), 3.69 (m, 4H), 3.73 (m, 4H), 3.77 (m, 4H), 3.82–3.85 (m, 8H), 4.04 (br s, 4H), 4.38 (br s, 4H), 7.19 (tt, 6H), 7.70 (dd, 12H), 7.83 (br s, 2H), 8.95–9.45 (br m, 8H);  $m/z$  (FAB) 2282, <sup>13</sup>C<sub>2</sub>C<sub>148</sub>H<sub>206</sub>N<sub>8</sub>O<sub>10</sub> (M<sup>+</sup> + H<sup>+</sup>) requires 2281.

The fourth fraction was collected and applied to a fresh silica column (eluent: toluene, 20 °C,  $R_f=0.2$ ) and recrystallised from heptane to afford 2,3,9,10-tetrakis(hexadecyl)-16(17),23(24)-bis(14,14,14-triphenyl-1,4,7,10,13-pentaoxatetradecyl)phthalocyanine **5** as a mixture of three isomers (268 mg, 7.0%). (Found C, 79.06; H, 9.12; N, 4.80%. C<sub>150</sub>H<sub>206</sub>N<sub>8</sub>O<sub>10</sub> requires C, 78.97; H, 9.10; N 4.80%);  $\lambda_{\text{max}}$  (CH<sub>2</sub>Cl<sub>2</sub>)/nm 706, 670, 638, 608, 380, 344, 292;  $\delta_{\text{H}}$  (500 MHz, C<sub>6</sub>D<sub>6</sub>, 60 °C) -1.10 (2H, br s), 1.00 (t, 12H), 1.34–1.89 (br m, 104H), 2.10–2.25 (br m, 8H), 3.26–3.40 (br m, 8H), 3.44 (m, 4H), 3.69 (m, 4H), 3.73 (m, 4H), 3.77 (m, 4H), 3.82–3.85 (m, 8H), 3.95–4.06 (br m, 4H), 4.34–4.50 (br m, 4H), 7.18 (tt, 6H), 7.70 (dd, 12H), 7.76 (br s, 2H), 8.95–9.65 (br m, 8H);  $m/z$  (FAB) 2283, <sup>13</sup>C<sub>2</sub>C<sub>148</sub>H<sub>206</sub>N<sub>8</sub>O<sub>10</sub> (M<sup>+</sup> + H<sup>+</sup>) requires 2281.

The fifth fraction was collected and applied to a fresh silica column (eluent: toluene-THF, 20:1, 20 °C,  $R_f=0.2$ ) and recrystallised from heptane to afford 2,3-bis(hexadecyl)-9(10),16(17),23(24)-tris(14,14,14-triphenyl-1,4,7,10,13-pentaoxatetradecyl)phthalocyanine **6** as a mixture of four isomers (298 mg, 8%). (Found C, 76.44; H, 7.38; N, 4.86%. C<sub>145</sub>H<sub>172</sub>N<sub>8</sub>O<sub>15</sub> requires C, 76.82; H, 7.65; N, 4.94%);  $\lambda_{\text{max}}$  (toluene)/nm 707, 671, 638, 610, 380, 344;  $\delta_{\text{H}}$  (500 MHz, C<sub>6</sub>D<sub>6</sub>, 60 °C) -1.45 (br s, 2H), 1.00 (t, 6H), 1.34–1.89 (br m, 52H), 2.15–2.23 (br m, 4H), 3.22–3.40 (br m, 4H), 3.44 (m, 6H), 3.68 (m, 6H), 3.74 (m, 6H), 3.77 (m, 6H), 3.82–3.85 (m, 12H), 3.90–4.08 (br m, 6H), 4.34–4.50 (br m, 6H), 7.18 (tt, 9H), 7.70 (dd, 18H), 7.76 (br m, 3H), 8.95–9.65 (br m, 8H);  $m/z$  (FAB) 2269, <sup>13</sup>C<sub>2</sub>C<sub>143</sub>H<sub>172</sub>N<sub>8</sub>O<sub>15</sub> (M<sup>+</sup> + H<sup>+</sup>) requires 2267.

The sixth fraction was collected and applied to a fresh silica column (eluent: toluene-THF, 10:1, 20 °C,  $R_f=0.2$ ) and recrystallised from heptane to afford 2,9(10),16(17),23(24)-tetrakis(14,14,14-triphenyl-1,4,7,10,13-pentaoxatetradecyl)phthalocyanine **7** as a mixture of four isomers (105 mg, 3%) (Found C, 74.33; H, 6.12; N, 5.01%. C<sub>140</sub>H<sub>138</sub>N<sub>8</sub>O<sub>20</sub> requires C, 74.65; H, 6.18; N, 4.97%);  $\lambda_{\text{max}}$  (toluene)/nm 704, 668, 646, 608, 384, 344;  $\delta_{\text{H}}$  (500 MHz, C<sub>6</sub>D<sub>6</sub>, 60 °C) -2.5 (br s, 2H), 3.45 (m, 8H), 3.70 (m, 8H), 3.76 (m, 8H), 3.81 (m, 8H), 3.89 (m, 16H), 4.00–4.15 (8H, br m), 4.32–4.51 (br m, 8H), 7.20 (tt, 12H), 7.71 (dd, 24H), 7.76 (br m, 4H), 8.82–9.51 (m, 8H);  $m/z$  (FAB) 2254, <sup>13</sup>CC<sub>138</sub>H<sub>138</sub>N<sub>8</sub>O<sub>20</sub> (M<sup>+</sup> + H<sup>+</sup>) requires 2254.

### 2,3,9,10,16,17-Hexakis(hexadecyl)-23-(12-hydroxy-1,4,7,10-tetraoxadodecyl)phthalocyanine 8

A solution of compound **3** (200 mg, 95  $\mu\text{mol}$ ), THF (30 ml) and hydrochloric acid (1 ml, 10 mol l<sup>-1</sup>) was heated at reflux

for 1 h. On cooling, the solvent was removed under reduced pressure and the resulting solid redissolved and eluted through a silica column (eluent: toluene–THF). Recrystallisation from heptane gave **8** as a blue solid (160 mg, 82%) (Found C, 79.81; H, 10.82; N, 5.40%.  $C_{136}H_{226}N_8O_5$  requires C, 79.94; H, 10.66; N, 5.49%);  $\lambda_{\max}$ (toluene)/nm 706, 670, 644, 606, 350;  $\delta_H$ (500 MHz,  $C_6D_6$ , 60 °C) –0.8 (br s, 2H), 1.00 (t, 18H), 1.22–1.7 (m, 144H), 1.78 (m, 12H), 2.14 (m, 12H), 3.33 (m, 12H), 3.51 (t, 2H), 3.61 (t, 2H), 3.66 (m, 2H), 3.73 (m, 2H), 3.82 (m, 2H), 3.98 (br t, 4H), 4.40 (br t, 2H), 7.82 (d, 1H), 9.08 (br s, 1H), 9.45–9.77 (br m, 7H), signal of hydroxy proton hidden by alkyl resonances.

### 2,3,16,17-Tetrakis(hexadecyl)-9,23-(12-hydroxy-1,4,7,10-tetraoxadodecyl)phthalocyanine **9**

Pc **9** was prepared from **4** by a similar procedure to that for **8** and recrystallised from toluene (39 mg, 62%) (Found C, 74.58; H, 9.71; N, 6.42%.  $C_{112}H_{178}N_8O_{10}$  requires C, 74.87; H, 9.99; N, 6.24%);  $\lambda_{\max}$ (toluene)/nm 708, 672, 642, 610, 384, 344;  $\delta_H$ (500 MHz,  $C_6D_6$ , 60 °C) –1.8 (br s, 2H), 1.00 (t, 12H), 1.30–1.89 (br m, 104H), 2.10–2.25 (br m, 8H), 3.10–3.43 (br m, 8H), 3.50 (m, 4H), 3.67 (m, 4H), 3.71 (m, 4H), 3.78 (m, 4H), 3.82–3.86 (m, 8H), 4.06 (br s, 4H), 4.45 (br s, 4H), 7.85 (br s, 2H), 8.85–9.45 (br m, 8H), signal of hydroxy proton hidden by alkyl resonances;  $m/z$  (FAB) 1796,  $^{13}C_2C_{110}H_{178}N_8O_{10}$  ( $M^+ + H^+$ ) requires 1797.

### 2,3,9,10-Tetrakis(hexadecyl)-16,23-bis(12-hydroxy-1,4,7,10-tetraoxadodecyl)phthalocyanine **10**

Pc **10** was prepared from **5** by a similar procedure to that for **8** and recrystallised from toluene (94 mg, 80%) (Found C, 74.59; H, 9.69; N, 6.04%.  $C_{112}H_{178}N_8O_{10}$  requires C, 74.87; H, 9.99; N 6.24%);  $\lambda_{\max}$ ( $CH_2Cl_2$ )/nm 706, 670, 638, 608, 384, 344, 292;  $\delta_H$ (500 MHz,  $C_6D_6$ , 60 °C) –1.40 (2H, br s), 1.00 (t, 12H), 1.34–1.89 (br m, 104H), 2.10–2.30 (br m, 8H), 3.26–3.40 (br m, 8H), 3.55 (m, 4H), 3.65 (m, 4H), 3.69 (m, 4H), 3.77 (m, 8H), 3.85 (m, 4H), 3.86 (br m, 4H), 4.00–4.50 (br m, 4H), 7.60–7.75 (br s, 2H), 8.75–9.65 (br m, 8H), signal of hydroxy proton hidden by alkyl resonances;  $m/z$  (FAB) 1797,  $^{13}C_2C_{110}H_{178}N_8O_{10}$  ( $M^+ + H^+$ ) requires 1797.

### 2,3-Bis(hexadecyl)-9,16,23-tris(12-hydroxy-1,4,7,10-tetraoxadodecyl)phthalocyanine **11**

Pc **11** was prepared from **6** by a similar procedure to that for **8** and recrystallised from toluene (79 mg, 68%) (Found C, 68.64; H, 8.34; N, 7.14%.  $C_{88}H_{130}N_8O_{15}$  requires C, 68.63; H, 8.51; N, 7.28%);  $\lambda_{\max}$ (toluene)/nm 706, 670, 638, 608, 384, 346, 292;  $\delta_H$ (500 MHz,  $C_6D_6$ , 60 °C) –3.3 (br s, 2H), 1.00 (t, 6H), 1.34–2.3 (br m, 52H), 2.80–3.31 (br m, 4H), 3.65 (m, 6H), 3.74 (m, 6H), 3.78 (m, 6H), 3.86 (m, 6H), 3.95 (m, 12H), 3.99–4.21 (br m, 6H), 4.30–4.58 (br m, 6H), 7.46–7.82 (br m, 3H), 8.00–9.65 (br m, 8H), signal of hydroxy proton hidden by alkyl resonances;  $m/z$  (FAB) 1541,  $^{13}C_2C_{86}H_{130}N_8O_{15}$  ( $M^+ + H^+$ ) requires 1541.

### 2,9,16,23-Tetrakis(12-hydroxy-1,4,7-tetraoxadodecyl)-phthalocyanine **12**

Pc **12** was prepared from **7** by a similar procedure to that for **8** and recrystallised from THF–toluene (45 mg, 65%) (Found C, 59.53; H, 6.59; N, 8.47%.  $C_{64}H_{82}N_8O_{20}$  requires C, 59.90; H, 6.44; N, 8.73%);  $\lambda_{\max}$ ( $CH_2Cl_2$ )/nm 704, 670, 646, 608, 384, 344;  $\delta_H$ (500 MHz,  $d_6$ -DMSO, 80 °C) –3.1 (br s, 2H), 3.50–3.60 (m, 8H), 3.70 (m, 8H), 3.75 (m, 8H), 3.85 (m, 8H), 3.94 (m, 8H), 4.20 (b m, 8H), 4.33 (b m, 8H), 4.66 (br m, 8H), 7.50–7.69 (b m, 4H), 8.10–8.29 (b m, 4H), 8.50–8.70 (br m, 4H), signal of hydroxy proton hidden by alkyl resonances;  $m/z$  (FAB) 1283,  $^{13}CC_{63}H_{82}N_8O_{20}$  ( $M^+ + H^+$ ) requires 1284.

## Results and discussion

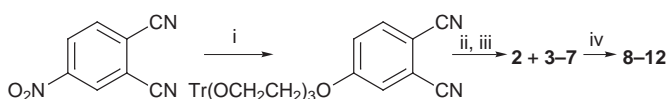
### Pc synthesis

Pcs **2–12** are prepared by the route shown in Scheme 1. An aromatic nucleophilic substitution reaction<sup>6f,12</sup> between tetraethylene glycol monotrityl ether and commercially available 4-nitrophthalonitrile provides the important precursor 4-(14,14,14-triphenyl-1,4,7,10,13-pentaoxatetradecyl)phthalonitrile **1**. The mixed cyclotramerisation of 4,5-bis-(hexadecyl)phthalonitrile and **1** gives a complex product mixture from which Pcs **2–7** are readily separated by simple column chromatography.<sup>6g</sup> The trityl protecting groups are removed from **2–7** under acid catalysed hydrolytic conditions to give the amphiphilic Pcs **8–12**, respectively. The structure and purities of Pcs **2–12** were confirmed by fast atom bombardment mass spectrometry (FABMS), high resolution  $^1H$  NMR (500 MHz) and UV–VIS absorption spectroscopy, elemental analysis and HPLC (purity >99%). NMR analysis is consistent with Pcs **4** and **9** being composed of a statistical mixture of two inseparable regioisomers and Pcs **5** and **10** being composed of three inseparable regioisomers. The separation of *opposite* (**4** and **9**) and *adjacent* (**5** and **10**) isomers containing both oligo(ethyleneoxy) and alkyl side chains has been demonstrated previously.<sup>6g</sup> Pc **8** is insufficiently soluble in cold solvents to allow investigations into the fabrication of LB and spin-coated films derived from this compound.

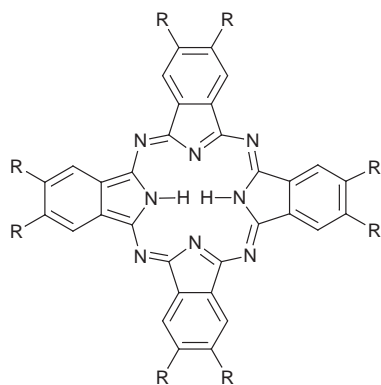
### Mesophase properties

All of the Pcs **2–12** display at least one thermotropic mesophase. The transition temperatures and enthalpies, as measured by differential scanning calorimeter (DSC), are given in Table 1. Polarising optical microscopy of these materials gave in total four distinct optical textures, only one of which is easily assigned as that of a columnar hexagonal mesophase [ $\phi_h$ ,<sup>13</sup> Fig. 1(a) and 2(a)]. Low resolution powder X-ray diffraction (XRD) studies of each Pc were carried out, however these failed to give adequate information for structural elucidation of the other mesophases. Therefore, high resolution measurements were made using a synchrotron X-ray source for Pcs **2** and **8–11**. These results and the low resolution data for Pcs **3–7** and **12** are collected in Table 2.

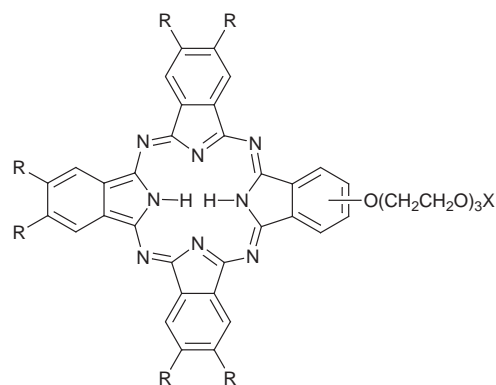
High resolution XRD measurements confirm that the symmetrical Pc **2** has two distinct mesophases. Previously there was some doubt as to whether the lower temperature mesophase of **2** was simply a textural variation of  $\phi_h$ ,<sup>6g</sup> in analogy with behaviour displayed by 1,4,8,11,15,18,22,25-octaalkyl-Pcs.<sup>15</sup> However, the two distinct small angle diffraction rings, observed by high resolution XRD, are assignable to diffraction from the 200 and 110 planes of a rectangular lattice. These reflections would be coincident for a hexagonal mesophase. The 'striated focal conic' optical texture [Fig. 1(b)] has been associated with a columnar rectangular mesophase with a  $P2_1/a$  plane group symmetry [ $\phi_{r(P2_1/a)}$ , Fig. 2(b)].<sup>14</sup> However, we did not observe a reflection from 210 for this or the lower temperature mesophase of amphiphilic Pcs **9** which also displays the striated focal conic texture. The lack of a reflection from the 210 plane suggests  $C2/m$  plane group symmetry [ $\phi_{r(C2/m)}$ , Fig. 2(c)], although it has been noted in previous studies of the  $\phi_{r(P2_1/a)}$  mesophase that diffraction from the 210 plane can be very weak and may not be



**Scheme 1** Reagents and conditions: i,  $Tr(OCH_2CH_2)_3OH$ , anhydrous  $K_2CO_3$ , DMF, 50–70 °C; ii, 4,5-Bis(hexadecyl)phthalonitrile, lithium, pentanol, 135 °C; iii, acetic acid, separation by chromatography; iv, HCl (aq), THF, reflux.

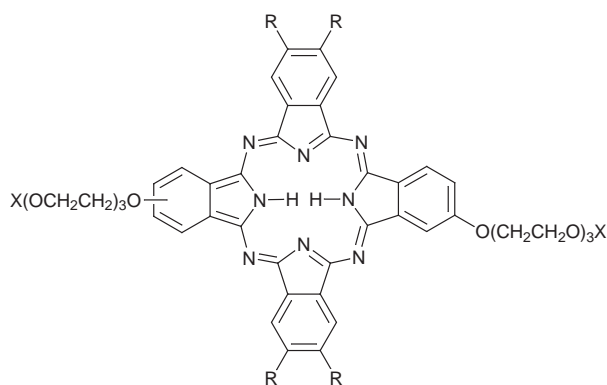


2 R = C<sub>16</sub>H<sub>33</sub>



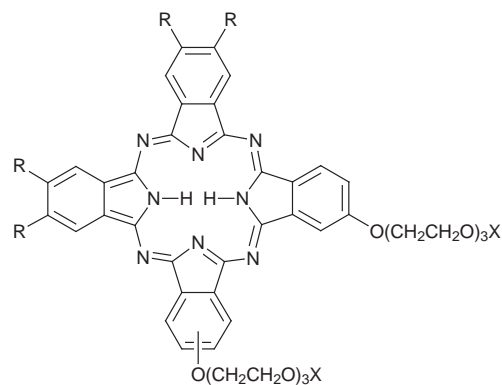
3 X = -Trityl, R = C<sub>16</sub>H<sub>33</sub>

8 X = -H, R = C<sub>16</sub>H<sub>33</sub>



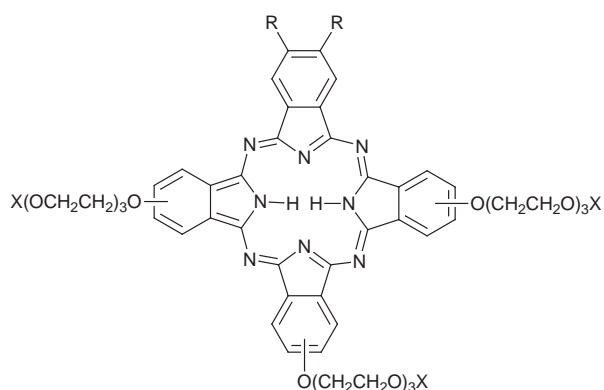
4 X = Trityl, R = C<sub>16</sub>H<sub>33</sub>

9 X = H, R = C<sub>16</sub>H<sub>33</sub>



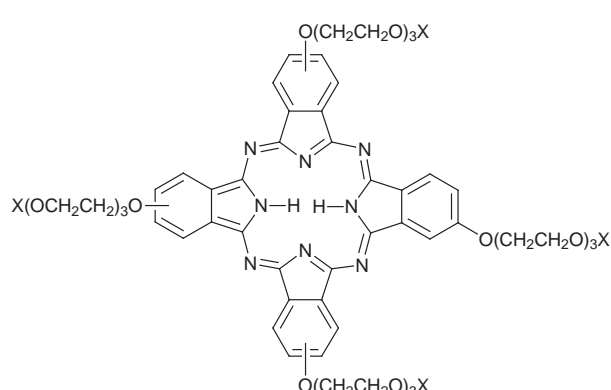
5 X = Trityl, R = C<sub>16</sub>H<sub>33</sub>

10 X = H, R = C<sub>16</sub>H<sub>33</sub>



6 X = Trityl, R = C<sub>16</sub>H<sub>33</sub>

11 X = H, R = C<sub>16</sub>H<sub>33</sub>



7 X = Trityl

12 X = H

discernible from the background 'noise'.<sup>16</sup> Therefore, we denote this mesophase simply as  $\varphi_{r1}$ . For the lower temperature mesophase of Pc **11**, which displays the striated focal conic texture of  $\varphi_{r1}$ , there is a weak diffraction assignable to the 210 plane suggesting  $P2_1/a$  symmetry. In addition, there is a strong diffraction ( $d$ -spacing = 54.0 Å) which appears to originate from the 100 plane of the rectangular lattice. Reflection from this plane is not consistent with the extinction rules<sup>17</sup> for a rectangular lattice of  $P2_1/a$  or  $C2/m$  plane symmetry group and suggests additional bilayer lamellar ordering. A much weaker reflection from the 100 plane is also observed in the  $\varphi_h$  mesophase of **11** perhaps resulting from the asymmetry of the molecule and indicating segregation of the two types of side-chain even at high temperature.

Pc **10** possesses exceptional mesophase behaviour. Most Pc mesogens have a  $\varphi_h$  mesophase over a broad temperature range

whereas **10** displays a monotropic  $\varphi_h$  which is stable over only a few degrees. The stable higher temperature mesophase of **10** has a 'mosaic' texture with large domain size [Fig. 1(c)]. High resolution XRD analysis allows assignment of some diffraction peaks to a rectangular lattice but additional small angle diffractions ( $d$ -spacings = 52.2 and 47.7 Å) may be due to a bilayer lamellar superstructure. This mesophase is denoted as  $\varphi_{r2}$ . The lower temperature mesophase of **10** is characterised by a granular texture [Fig. 1(d)] superimposed on the mosaic texture of the  $\varphi_{r2}$  mesophase on cooling. We initially described this as a bilayer lamellar mesophase ( $\varphi_L$ ) on the basis of low resolution XRD analysis and the pronounced lamellar self-ordering properties of this compound.<sup>7</sup> However, high resolution XRD shows diffractions originating from further ordering ( $d$ -spacings = 47.2 and 23.7 Å) in addition to the stronger lamellar diffractions ( $d$ -spacings = 57.2, 28.6 and 19.2 Å).

**Table 1** Mesophase transition temperatures (°C) with enthalpy changes ( $\Delta H/J\text{ g}^{-1}$ ) in parentheses. K = crystal,  $\phi_L$  = columnar lamellar mesophase,  $\phi_{r1}$  = columnar rectangular mesophase which displays striated focal conic texture [Fig. 1(b)],  $\phi_{r2}$  = columnar rectangular mesophase which displays mosaic texture [Fig. 1(c)];  $\phi_h$  = columnar hexagonal mesophase. Transition temperature and enthalpies for the heating cycle.

Pc	Glass- $\phi_h$	K- $\phi_L$	K- $\phi_h$	K- $\phi_{r1}$	$\phi_{r1}$ - $\phi_h$	$\phi_L$ - $\phi_{r2}$	$\phi_{r2}$ -I	$\phi_h$ -I
2	—	—	—	108 (96)	170 <sup>a</sup>	—	—	196 (6)
3	—	—	—	86 (120)	89 <sup>a</sup>	—	—	167 (3)
4	—	—	—	41 (81)	191 (1)	—	—	196 (3)
5	—	—	—	77 (88)	—	—	—	152 (3)
6	—	—	—	32 (23)	76 (1)	—	—	177 (1)
7	30 <sup>b</sup>	—	—	—	—	—	—	225 (1)
8	—	—	—	81 (120)	107 (2)	—	—	189 (3)
9	—	—	—	71 (30)	109 (3)	—	—	234 (5)
10 <sup>c</sup>	—	79 (88)	—	—	—	132 (1)	194 (4)	—
11	—	—	—	80 (16)	252 (1)	—	—	273 (1)
12	—	—	75 (14)	—	—	—	—	>320

<sup>a</sup>Transition not observed by DSC. <sup>b</sup>Glass transition temperature. <sup>c</sup>Pc 10 also displays a monotropic  $\phi_h$  mesophase on cooling from the isotropic liquid.

All of the Pc mesophases display broad wide-angle diffraction rings correlating to  $d$ -spacings of 4–5 Å. The mesophases of Pcs 6, 7, 11 and 12 display an additional sharp wide angle diffraction ring corresponding to 3.5 Å which indicates an untilted columnar structure in which there is significant

cofacial ordering of the Pc molecules within the molecular stacks. Previous studies have suggested that alkoxy substituted Pc mesogens are able to form relatively ordered columnar structures due to the smaller steric demand of the oxygen linking group as compared to the methylene group of alkyl

**Table 2** Powder X-ray diffraction data for Pcs 2–12. Each diffraction is given in Ångstrom units. For each mesophase the assignments are based on a rectangular lattice, but for the mesophase and solid phase assignments of Pcs 9–11 a lamellar structure is also considered.

Pc	Phase $T/^\circ\text{C}$	Observed $d$ -spacings/Å (assignments)				2-D lattice dimensions/Å		
2 <sup>a</sup>	$\phi_h$ (190)	30.0 (110/200)	17.3 (310/020)	15.0 (400/220)	4–5			$b=34.6$ $a=\sqrt{3}b$
	$\phi_{r1}$ (140)	31.3 (200)	28.9 (110)	18.3 (310)	16.3 (020)	4–5		$a=62.6$ $b=32.5$
3 <sup>b,c</sup>	$\phi_h$ (120)	29.2 (110/200)	16.8 (310/020)	14.3 (400/220)	4–5			$b=33.7$ $a=\sqrt{3}b$
	5 <sup>b</sup>	$\phi_h$ (120)	29.5 (110/200)	17.0 (310/020)	14.6 (400/220)	4–5		$b=34.1$ $a=\sqrt{3}b$
6 <sup>b</sup>	$\phi_h$ (130)	29.6 (110/200)	16.8 (310/020)	14.3 (400/220)	4–5	3.5		$b=34.2$ $a=\sqrt{3}b$
	$\phi_{r1}$ (60)	28.5 (200)	23.1 (110)	15.1 (310)	4–5	3.5		$a=57.0$ $b=25.3$
7 <sup>b</sup>	$\phi_h$ (120)	28.5 (110/200)	16.9 (310/020)	14.3 (400/220)	4–5	3.5		$b=32.9$ $a=\sqrt{3}b$
	glass (25)	8.5 (110/200)	16.9 (310/020)	14.3 (400/220)	4–5	3.5		$b=32.9$ $a=\sqrt{3}b$
8 <sup>b</sup>	$\phi_h$ (150)	28.5 (110/200)	16.6 (310/020)	14.3 (400/220)	4–5			$b=32.9$ $a=\sqrt{3}b$
	$\phi_{r1}$ (100)	30.8 (200)	28.5 (110)	18.0 (310)	16.0 (020)	4–5		$a=61.6$ $b=32.1$
9 <sup>a</sup>	$\phi_h$ (200)	29.7 (110/200)	17.1 (310/020)	15.1 (400/220)	4–5			$b=34.3$ $a=\sqrt{3}b$
	$\phi_{r1}$ (90)	27.9 (200)	23.1 (110)	15.0 (310)	4–5			$a=55.8$ $b=25.4$
10 <sup>a</sup>	Solid (25)	29.8 ( $n=1$ )	15.1 ( $n=2$ )	4–5				$L=29.8$
	$\phi_{r2}$ (180)	52.2 (100, $n=1$ )	47.7 (?)	28.5 (110)	21.0 (210)	16.8 (020)	4–5	$a=52.2$ $b=34.0$ $(L=52.2)$
11 <sup>a</sup>	$\phi_L$ (120)	57.2 ( $n=1$ )	47.2 (?)	28.6 ( $n=2$ )	23.7 (?)	19.2 ( $n=3$ )	4–5	$L=57.2$
	Solid (25)	50.2 ( $n=1$ )	46.5 (?)	25.4 ( $n=2$ )	16.8 ( $n=3$ )	4–5		$L=50.2$
12 <sup>b</sup>	$\phi_h$ (265)	53.0 (100, $n=1$ )	26.5 (110/200)	15.3 (310/020)	4–5	3.5		$b=30.6$ $a=\sqrt{3}b$ $(L=53)$
	$\phi_{r1}$ (230)	54.0 (100, $n=1$ )	27.2 (200, $n=2$ )	25.5 (110)	19.5 (210)	17.6 (300, $n=3$ )	3–5	$a=54.0$ $b=28.8$ $(L=54.0)$
	Solid (30)	51.8 ( $n=1$ )	26.0 ( $n=2$ )	17.3 ( $n=3$ )	4–5	3.5		$(L=51.8)$
	$\phi_h$ (200)	23.0 (110/200)	4–5	3.5				$b=26.6$ $a=\sqrt{3}b$

<sup>a</sup>High resolution XRD using SRS. <sup>b</sup>Low resolution XRD. <sup>c</sup>Lower temperature mesophase is stable over too small a range for XRD analysis on low resolution equipment.



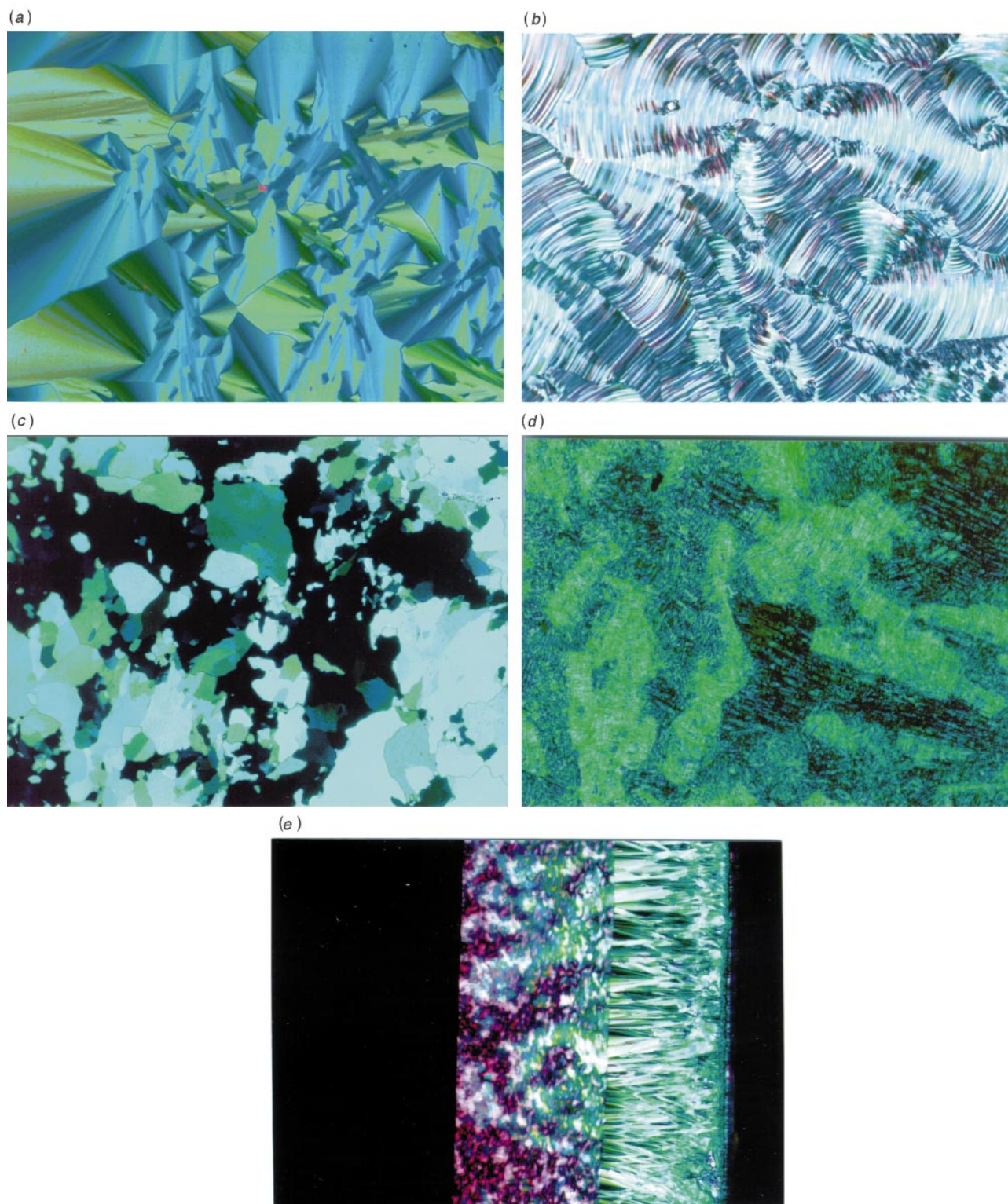


**Fig. 1** The optical texture of (a) the  $\phi_h$  mesophase (Pc **2**, 187 °C), (b) the  $\phi_{r1}$  mesophase (Pc **2**, 160 °C), (c) the  $\phi_{r2}$  mesophase (Pc **10**, 150 °C), (d) the  $\phi_L$  mesophase (Pc **10**, 120 °C) and (e) the lyotropic  $N_c$  mesophase of Pc **12** which appears between the isotropic dilute ethanolic solution and the pure material (right of micrograph). All textures observed through crossed polarisers at a magnification of  $\times 100$ .

substituted Pcs.<sup>16</sup> The wide-angle XRD results of Pcs **6** and **11** suggest that two alkyl substituents are insufficient to reduce the intermolecular ordering within the columnar mesophase.

Pc **7** forms an anisotropic glass, on cooling from the mesophase, in which the ordered structure of the  $\phi_h$  mesophase is frozen. DSC shows clearly the reversible glass transition and XRD indicates the hexagonal columnar structure of the resulting brittle solid.<sup>18</sup> The bulky nature of the four large trityl end-groups appears responsible for this behaviour.

Similar anisotropic glass formation has been described recently for Pcs containing large dendritic substituents.<sup>19</sup>

Pc **12** is soluble in protic polar solvents such as ethanol. The analysis of concentrated ethanolic solutions of Pc **12** by polarising optical microscopy shows a ‘marbled’ texture [Fig. 1(e)] which is one of the characteristic textures of the columnar nematic lyotropic mesophase [ $N_c$ ; Fig. 2(d)].<sup>1f</sup> UV–VIS analysis of dilute ethanolic solutions of Pc **12** ( $\lambda_{\max} = 620$  nm) indicates the presence of the columnar aggre-

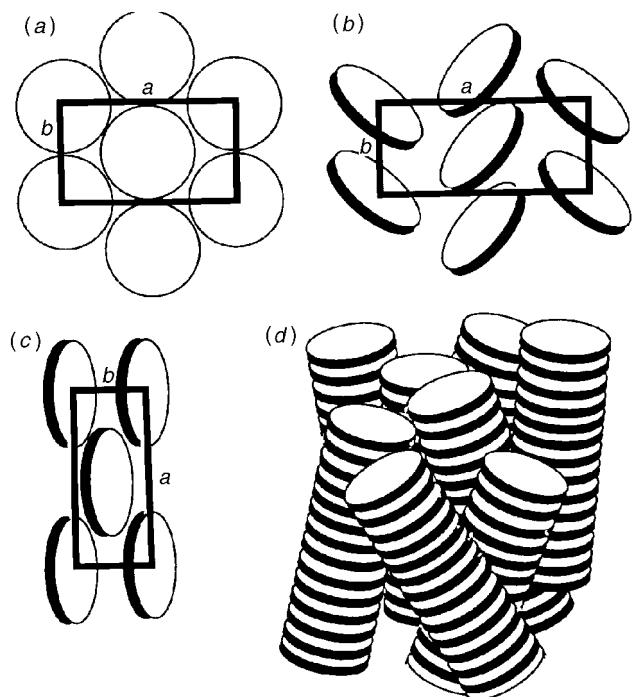


**Fig. 2** (a) Columnar hexagonal mesophase ( $\phi_h$ ,  $a = \sqrt{3}b$ ), (b) columnar rectangular mesophase with  $P2_1/a$  plane group symmetry, (c) rectangular disordered with  $C2/m$  plane group symmetry and (d) columnar nematic mesophase ( $N_c$ ).

gates which are a prerequisite for the formation of the  $N_c$  mesophase.

#### Langmuir–Blodgett film forming properties

The LB technique, which involves film fabrication by the sequential deposition of a monolayer formed at an air–water interface, has been thoroughly investigated as a method of preparing multilayer films derived from soluble Pc derivatives.<sup>1a,4</sup> It is apparent that an amphiphilic character is highly advantageous for obtaining a truly ordered multilayer film.<sup>4d–f</sup> Thus, the LB film forming properties of soluble amphiphilic Pcs **9**, **10** and **11** were studied.

Table 3 summarises the important Langmuir isotherm parameters of area per molecule extrapolated to a surface pressure of  $0 \text{ mN m}^{-1}$  ( $A_0$ ), the area per molecule at a surface pressure of  $30 \text{ mN m}^{-1}$  ( $A_{30}$ ) and the collapse pressure ( $\pi_c$ ) for the monolayer. For each Pc these figures are consistent with the formation of a stable molecular monolayer at the air–water interface in which the Pc molecules are oriented approximately perpendicular to the water surface. For Pc **10**, assuming that both hydrophilic tetra(ethyleneoxy) chains are immersed in the water, the effective area per molecule would be determined by the four hydrophobic hexadecyl chains. This value can be estimated as  $155 \text{ \AA}^2$  from the intercolumnar distance ( $35.5 \text{ \AA}$ ) and the cofacial intermolecular distance ( $4.5 \text{ \AA}$ ) of the hexagonal mesophase of symmetrical Pc **2** (Table 2). Similarly for Pc **11**, assuming that all three tetra(ethyleneoxy) chains are immersed in the water, the effective

**Table 3** The monolayer (Langmuir isotherm) properties of the amphiphilic Pcs **9–11** at the air–water interface. The estimated values for the molecular area ( $A_{\text{est}}$ ) are derived from the appropriate XRD data (see text).

Pc	$A_0/\text{\AA}^2$	$A_{30}/\text{\AA}^2$	$A_{\text{est}}/\text{\AA}^2$	$\pi_c/\text{mN m}^{-1}$
<b>9</b>	154	140	155	43
<b>10</b>	143	122	155	49
<b>11</b>	99	85	93	53

area per molecule can be estimated as  $93 \text{ \AA}^2$  from the intercolumnar distance ( $26.5 \text{ \AA}$ ) and the cofacial intermolecular distance ( $3.5 \text{ \AA}$ ) of the hexagonal mesophase of Pc **12** (Table 2). These estimated areas per molecule ( $A_{\text{est}}$ ) are in reasonable agreement with the observed values of  $A_0$  and  $A_{30}$  for Pcs **10** and **11** (Table 3). The observed values of  $A_0$  and  $A_{30}$  for Pc **9** (Table 3) also imply a perpendicular orientation of the Pc molecules in its monolayer (estimated area =  $155 \text{ \AA}^2$ ) rather than a parallel orientation (estimated minimum area =  $225 \text{ \AA}^2$ ) that would allow both tetra(ethyleneoxy) side-chains to be immersed simultaneously. For Pcs **9**, **10** and **11** the Langmuir isotherms are characterised by a lack of hysteresis and good monolayer stability for prolonged periods of time at a surface pressure of  $30 \text{ mN m}^{-1}$ .

Despite these encouraging monolayer properties, multilayer films of Pcs **9**, **10** and **11** could not be deposited onto either hydrophilic or hydrophobic substrates. In each case, successful deposition on the up stroke was followed by the loss of the material on the down stroke. This was the case even after allowing the initially deposited monolayer to dry for over 1 h. It should be noted that conventional oligo(ethyleneoxy)-based non-ionic surfactants are also poor LB film forming materials.<sup>20</sup>

#### Order in solvent cast and spin-coated films

The simple process of forming films cast from chloroform solutions ( $20 \text{ mg ml}^{-1}$ ) of Pcs **9**, **10** and **11** onto clean, hydrophobic substrates gives films with a high degree of lamellar ordering—as indicated by glancing angle XRD. Films cast onto hydrophilic substrates show no evidence of a lamellar structure, suggesting that in the ordered films the non-polar hexadecyl side-chains of the first monolayer are in contact with the surface of the substrate. For the cast films of Pcs **10** and **11**, the large  $d$ -spacings are consistent with a bilayer structure in which the Pc molecules are oriented perpendicular to the surface of the substrate. Pc **9** gives a cast film for which the  $d$ -spacing is consistent with a monolayer structure (Table 4). The formation of a bilayer from Pc **9** is disfavoured by its substitution pattern which places side-chains of similar polarity on opposite sides of the molecule. The apparent degree of ordering within these films can be increased by annealing for a short time at a temperature at which the material is mesogenic (Fig. 3, Table 4).<sup>7</sup> However, these solvent cast films are of non-uniform thickness. A number of recent studies have indicated that spin coating is a useful technique for the preparation of films of uniform thickness derived from soluble Pcs.<sup>5</sup> These films proved to be amorphous or microcrystalline in structure.

Spin-coated films of Pcs **9–11** on hydrophobic substrates do not show any evidence of long-range order by glancing angle XRD and the films appear non-birefringent by polarising optical microscopy. Annealing the films for a short period of time at a temperature at which the Pc is liquid crystalline

**Table 4** Glancing angle XRD data for solvent cast and spin coated films of Pcs **9–11** after annealing in their mesophase

Pc	Film fabrication	Lamellar $d$ -spacing/ $\text{\AA}$	Orders of diffraction	Intensity <sup>a</sup> (arbitrary units)
<b>9</b>	cast	29.5	2	838
<b>9</b>	spin coated	30.2	2	120 <sup>b</sup>
<b>10</b>	cast	49.7	4	458
<b>10</b>	spin coated	48.6	3	85 <sup>b</sup>
<b>11</b>	cast	51.3	5	813 <sup>c</sup>
<b>11</b>	spin coated	50.0	5	155 <sup>b,c</sup>

<sup>a</sup>Intensity of the first order diffraction peak. <sup>b</sup>The spin coated films are significantly thinner than the solvent cast films, which may account for the lower intensity of the diffraction peaks from these film. <sup>c</sup>Second order diffraction peak is more intense by  $\sim 20\%$ .

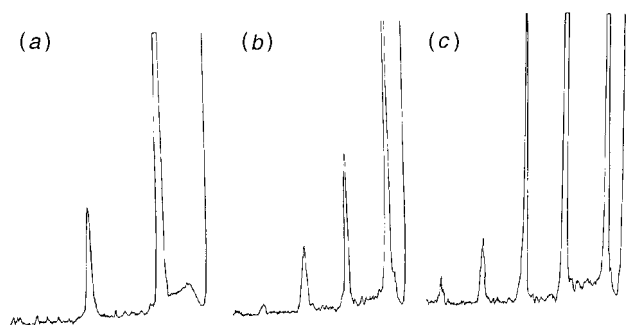


Fig. 3 Glancing angle X-ray diffractograms from the solvent cast films of Pcs (a) **9**, (b) **10** and (c) **11** after heating at a temperature at which the Pc displays a columnar mesophase.

results in the formation of highly ordered films which possess both the lamellar structure of the solvent cast films (Table 4) and the uniform thickness of the unannealed spin-coated films. As such, these films are reminiscent of LB multilayers but are much easier to fabricate. There is reasonable agreement between the lamellar spacings in the annealed films, solid and lower temperature mesophases for Pcs **9–11** (Table 2 and 4). Clearly, the attainment of high lamellar order during annealing is due to the self-ordering within the lower temperature mesophase of the Pc resulting in segregation of the non-polar hexadecyl side-chains from the polar hydroxy terminated tetra(ethyleneoxy) side-chains. Similar effects have been observed in solvent cast films composed of other types of amphiphilic molecules such as phospholipids.<sup>21</sup> UV-VIS spectra of the annealed films derived from Pcs **9–11** show that the major absorption (Q-band) is at 620 nm, shifted by exciton interactions to a lower wavelength compared to the main absorption band of their solution spectra ( $\lambda_{\text{max}} = 704$  nm), indicating that the Pc molecules are in a columnar arrangement within the solid lamellar structure.<sup>7</sup>

## Conclusions

The combination of spin-coating technology with mesomorphic ordering can produce highly ordered and uniform films of non-uniformly substituted Pcs **9–11**. The antipathy of two types of side-chains which have different polarity induces lamellar ordering both within the columnar liquid crystal and the solid phase of these derivatives. This phenomenon can be used to form self-ordering spin-coated films which display the structure and uniformity of idealised LB films. Despite the structural control offered by the LB technique and the intense research activity related to the possible applications of LB films over the past 15 years, the commercial exploitation of functional LB films composed of Pcs is unlikely. This is due to the prohibitively slow speed of deposition and the small area of substrate that can be covered. Self-ordering spin-coated films, such as described above, offer a rapidly fabricated alternative.

We thank the EPSRC for financial support (G.J.C.), provision of studentships (K.E.T., A.S.S.T.) and for allocation of beam time at Daresbury (S.R.S.).

## References

- 1 (a) N. B. McKeown, *Phthalocyanine Materials: Synthesis, Structure and Function*, Cambridge University Press, Cambridge, 1998; (b) C. C. Leznoff and A. B. P. Lever, *Phthalocyanines: Properties and Applications*, vols. 1–4, VCH, New York, 1989, 1993, 1993, 1997; (c) H. Schultz, H. Lehmann, M. Rein and

- M. Hanack, *Struc. Bonding*, 1991, **74**, 41; (d) C. Van Nostrum and R. J. M. Nolte, *Chem. Commun.*, 1996, 2385.
- 2 S. Dogo, J. P. Germain, C. Maleysson and A. Pauly, *Thin Solid Films*, 1992, **219**, 244.
- 3 N. Minami, K. Sasaki and K. Tsuda, *J. Appl. Phys.*, 1983, **54**, 6764.
- 4 (a) R. H. Tredgold, *Order in Thin Organic Films*, Cambridge University Press, Cambridge, 1994; (b) A. Ulman, *Introduction to Ultrathin Organic Films*, Academic Press, San Diego, 1991; (c) S. Baker, M. C. Petty, G. G. Roberts, M. V. Twigg, *Thin Solid Films*, 1983, **99**, 53; (d) M. J. Cook, M. F. Daniel, K. J. Harrison, N. B. McKeown and A. J. Thomson, *J. Chem. Soc., Chem. Commun.*, 1987, 1148; (e) J. D. Shutt, D. A. Batzel, R. V. Sudiwala, S. E. Rickert and M. E. Kenney, *Langmuir*, 1988, **4**, 1240; (f) N. B. McKeown, M. J. Cook, A. J. Thomson, K. J. Harrison, M. F. Daniel, R. M. Richardson and S. J. Roser, *Thin Solid Films*, 1988, **159**, 469; (g) P. A. Albouy, *J. Phys. Chem.*, 1994, **98**, 8543; (h) M. Burghard, M. Schmelzer, S. Roth, P. Haisch and M. Hanack, *Langmuir*, 1994, **10**, 4265.
- 5 S. M. Critchley, M. R. Willis, M. J. Cook, J. McMurdo and Y. Maruyama, *J. Mater. Chem.*, 1992, **2**, 157; S. M. Critchley, M. R. Willis, Y. Maruyama, S. Bandow, M. J. Cook and J. McMurdo, *Mol. Cryst. Liq. Cryst.*, 1993, **230**, 287; M. J. Cook, *J. Mater. Chem.*, 1996, **6**, 677.
- 6 (a) J. Simon and C. Piechocki, *J. Am. Chem. Soc.*, 1982, **104**, 5245; (b) M. J. Cook, M. F. Daniel, K. J. Harrison, N. B. McKeown and A. J. Thomson, *J. Chem. Soc., Chem. Commun.*, 1987, 1086; (c) K. Ohta, L. Jacquemin, C. Sirlin, L. Bosio and J. Simon, *New J. Chem.*, 1988, **12**, 751; (d) J. F. Van der Pol, E. Neeleman, J. W. Zwikker, R. J. M. Nolte, W. Drenth, J. Aerts, R. Visser and S. J. Picken, *Liq. Cryst.*, 1989, **6**, 577; (e) A. N. Cammidge, M. J. Cook, K. J. Harrison and N. B. McKeown, *J. Chem. Soc., Perkin Trans. 1*, 1991, 3053; (f) N. B. McKeown and J. Painter, *J. Mater. Chem.*, 1994, **4**, 209; (g) G. J. Clarkson, N. B. McKeown and K. E. Treacher, *J. Chem. Soc., Perkin Trans. 1*, 1995, 1817; (h) G. J. Clarkson, B. M. Hassan, D. R. Maloney and N. B. McKeown, *Macromolecules*, 1996, **29**, 1854.
- 7 K. E. Treacher, G. J. Clarkson, Z. Ali-Adib and N. B. McKeown, *Chem. Commun.*, 1996, 73.
- 8 W. Bras, G. E. Derbyshire, A. J. Ryan, G. R. Mant, P. Manning, R. E. Cameron and W. Mormann, *J. Phys.*, 1993, **3**, 447; A. S. Stennett, PhD thesis, University of Manchester (UK), 1998.
- 9 F. Davies, P. Hodge, C. R. Towns and Z. Ali-Adib, *Macromolecules*, 1991, **24**, 5695.
- 10 D. D. Perrin and W. L. F. Armarego, *Purification of Laboratory Chemicals*, 3rd edn., Pergamon, Oxford, 1988.
- 11 N. Jayasuriya, S. Bosak and S. L. Regen, *J. Am. Chem. Soc.*, 1990, **112**, 5844.
- 12 W. O. Siegl, *J. Heterocycl. Chem.*, 1981, **18**, 1613; A. W. Snow and N. L. Jarvis, *J. Am. Chem. Soc.*, 1984, **106**, 4706; M. D. Pace, W. R. Barger and A. W. Snow, *Langmuir*, 1989, **5**, 973; S. M. Marcuccio, P. I. Svirskaya, S. Greenberg, A. B. P. Lever and K. B. Tomer, *Can. J. Chem.*, 1985, **63**, 3057; C. C. Leznoff, S. Greenberg, S. M. Marcuccio, P. C. Minor, P. Seymour and A. B. P. Lever, *Inorg. Chim. Acta*, 1984, **89**, L35.
- 13 The symbol  $\phi$  has recently become the accepted abbreviated notation for a columnar mesophase and has replaced the previously used D (discotic) nomenclature proposed in ref. 14.
- 14 C. Destrade, P. Foucher, H. Gasparoux, N. H. Tinh A. M. Levelut and J. Malthete, *Mol. Cryst. Liq. Cryst.*, 1984, **106**, 121.
- 15 A. S. Cherodian, A. N. Davies, R. M. Richardson, M. J. Cook, N. B. McKeown, A. J. Thomson, J. Feinjoo, G. Ungar and K. J. Harrison, *Mol. Cryst. Liq. Cryst.*, 1991, **196**, 103.
- 16 P. Weber, D. Guillon and A. Skoulios, *Liq. Cryst.*, 1991, **9**, 369; A. N. Cammidge, M. J. Cook, S. D. Haslam, R. M. Richardson and K. J. Harrison, *Liq. Cryst.*, 1993, **14**, 1847; N. Spielberg, M. Sarkar, Z. Lutz, R. Poupko, J. Billard and H. Zimmermann, *Liq. Cryst.*, 1993, **15**, 311.
- 17 T. Komatsu, K. Ohta, T. Watanabe, H. Ikemoto, T. Fujimoto and I. Yamamoto, *J. Mater. Chem.*, 1994, **4**, 537.
- 18 K. E. Treacher, G. J. Clarkson and N. B. McKeown, *Liq. Cryst.*, 1995, **19**, 887.
- 19 M. Brewis, G. J. Clarkson, A. M. Holder and N. B. McKeown, *Chem. Commun.*, 1998, 969.
- 20 M. J. Schtick, *Nonionic Surfactants: Physical Chemistry*, Marcel Dekker, New York, 1987.
- 21 T. Kunitake, *Angew. Chem., Int. Ed. Engl.*, 1992, **31**, 709.